Cryogenics 131 (2023) 103667

Contents lists available at ScienceDirect

Cryogenics

journal homepage: www.elsevier.com/locate/cryogenics

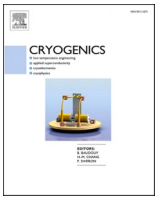

Thermodynamic optimization of 10–30 kA gas-cooled current leads with REBCO tapes for superconducting magnets at 20 K

Ho-Myung Chang [a], Na Hyeon Kim [a,*], Sangjun Oh [b]

[a] Hong Ik University, Seoul 04066, South Korea
[b] Korea Institute of Fusion Energy, Daejeon 34133, South Korea

ARTICLE INFO

Keywords:
Thermodynamics
Optimization
Current leads
REBCO
HTS magnet

ABSTRACT

Thermodynamic optimization is carried out to minimize the refrigeration work of gas-cooled current leads at a current level of 10–30 kA for superconducting magnets at 20 K. The binary HTS lead is a serial combination of REBCO (rare-earth barium copper oxide) tapes as cold part and copper conductor as warm part. In gas-cooled leads, liquid nitrogen is not used, but cold helium gas is supplied for forced-flow cooling through the channel between spiral fins of copper conductor. A special attention is paid to the conditions of gas-cooling, which can be integrated with a closed refrigeration cycle without any heat intercept or boil-off loss of liquid. The input power for refrigeration is rigorously calculated with the temperature-dependent properties of conductors. When a safety margin is selected on the critical current of REBCO, it is proven that there exists a unique optimum in the cooling-gas temperature and the dimensional size of copper conductor to minimize the required work for refrigeration. The results are compared with the optimized cases of conduction-cooled and vapor-cooled binary leads for 20 K magnets. The details of optimization procedure and design data are presented for practical application.

1. Introduction

The optimization of current leads is a significant thermodynamic subject for efficient refrigeration of superconducting systems [1–3]. The optimized leads are especially important in high-field magnets, because the large-current leads are a major source of cryogenic cooling load. Over decades, it has been verified that the input power for cryogenic refrigeration could be minimized by optimization, taking into consideration the thermo-electric properties of conductor materials and the cooling configuration [4–6]. Copper (Cu) is an excellent conductor at cryogenic temperatures, and therefore the most common lead material. Lately, HTS (high temperature superconductor) is used as the cold part of binary (HTS + Cu) leads [7–27] to take advantage of its low thermal conductivity. The recent success of second-generation REBCO (rare-earth barium copper oxide) tapes has expanded a new horizon of reliable lead material [12,15,17,21–25] as well as the conductor of HTS magnets.

This study is motivated by a five-year (2022–26) governmental project to develop the core technologies of high-field HTS magnets over 20 T, aiming at the immediate and practical application, for example, to nuclear fusion, NMR (nuclear magnetic resonance), or large accelerator magnets. In these emerging HTS systems, the current level is typically over 10 kA, and the operating temperature is expected to be around 20 K, considering the compactness and efficiency at the same time [28]. Towards the application, this paper begins with a variety of cooling options in the current leads for HTS magnets at 20 K, and proceeds to a comprehensive optimization of 10–30 kA gas-cooled leads with REBCO tapes.

Fig. 1 shows schematically five different options in conductor material and cooling configuration. Fig. 1(a) is the simple case of conduction-cooled Cu lead. The optimization principle is straight and clear, as derived earlier [4–6] to minimize the heat flow to cold end. There exists an optimum for the lead parameter (I/A) or the product of conductor length and current density to keep a balance between thermal conduction and Joule heating. The minimum work for refrigeration could be a criterion for comparing different options from thermodynamic point of view, as demonstrated later.

Heat intercept or multi-stage cooling is an effective method to reduce the input power for refrigeration [1,4–6,9,29]. Fig. 1(b) shows a two-stage conduction-cooled Cu lead. The work for refrigeration can be considerably reduced by heat intercept at an optimal location and temperature. Fig. 1(c) shows a conduction-cooled binary (REBCO + Cu) lead with heat intercept at the joint of two conductors [8,9]. The upper

* Corresponding author.
E-mail address: knahy@naver.com (N.H. Kim).

https://doi.org/10.1016/j.cryogenics.2023.103667
Received 6 January 2023; Received in revised form 10 March 2023; Accepted 19 March 2023
Available online 29 March 2023

Nomenclature

A	Cross-sectional area [cm^2]
C_p	Specific heat of He gas [kJ/kg-K]
Ch	Convective heat transfer (Chang) number
D	Diameter of conductor [cm]
d	Hydraulic diameter of cooling channel [cm]
h	Convection heat transfer coefficient [W/m^2-K]
I	Operating current [kA]
i	Specific enthalpy [kJ/kg]
k	Thermal conductivity [W/m-K]
L	Axial length of conductor [m]
L_0	Lorenz number [$W{\cdot}\Omega/K^2$]
$\dot{m}$	Mass flow rate of He gas [kg/s]
N	Number of REBCO tapes for stack
P	Perimeter of cooling channel [cm]
p	Fin pitch [mm]
Pr	Prandtl number of He gas
$\dot{Q}$	Heat flow [kW]
Re	Reynolds number of He gas
s	Specific entropy [kJ/kg-K]
T	Temperature [K]
t	Fin thickness [mm]
$\dot{W}$	Work rate or power [kW]
x	Axial distance from cold end

Greek letters

η_f	Fin efficiency
μ	Viscosity of He gas [$Pa{\cdot}s$]
ρ	Electrical resistivity of conductor [$\Omega{\cdot}m$]

Subscripts

1	REBCO tape
2	Cu conductor
e	Exit of He gas or effective perimeter
f	Fin
g	He gas
H	Warm end of Cu
i	Inlet of He gas or inner diameter
J	Joint of REBCO and Cu
L	Cold end of current lead
o	Outer diameter
rev	Reversible

Cu part could be optimized by itself, while the lower REBCO part should be designed with a safety margin to the critical current of REBCO tapes. The conduction-cooled binary leads are suitable for low-current (typically under 1 kA) systems, as conveniently integrated with commercial cryocoolers (based on Stirling, Gifford-McMahon, or pulse-tube cycle) [10] with a refrigeration capacity up to a few hundred Watts at 20–80 K.

In most binary leads for high-current systems at 4–5 K, Cu conductor is vapor-cooled, as shown in Fig. 1(d). The joint is cooled by liquid nitrogen and the boil-off vapor flows along the Cu conductor for convective cooling. The same configuration may be applied to high-current systems at 20 K as well. The vapor-cooled leads can be quickly designed with the assumption that the convective heat transfer is perfect or the temperatures of vapor and conductor are same at any axial location [2]. The assumption of perfect heat transfer is difficult to realize in practice, but a variety of design efforts have been made for effective convection with extended surface (such as spiral fins [14,17,18,25,27,30–32] or pierced sheets [11,20]) or flow control (such as flow agitators [4] and tortuous passages [20,23,24]). It was reported in [31] how the actual convection heat transfer affects the optimization in terms of dimensionless variable in liquid-helium or liquid-nitrogen systems.

Lately for high-current systems, a number of 10–30 kA gas-cooled binary leads have been developed [13–16,17,18,23–27], as shown in Fig. 5(e). The gas-cooled leads have a similar configuration with the vapor-cooled leads in a sense that the REBCO tapes are conduction-cooled and the Cu conductor is convection-cooled. The main difference is that cold gas is supplied for forced-flow by a refrigerator, therefore the joint temperature may be different from liquid-nitrogen temperature (77 K). It is also noted that the flow rate and inlet temperature of cooling gas can be independently selected in gas-cooled leads, while the boil-off rate is basically determined by the heat flow to liquid in vapor-cooled leads. One of the motivations to employ the gas-cooled leads is the possible integration with helium Brayton refrigerator [34] towards a fully closed system without any liquid supply or boil-off loss.

Although numerous recent efforts have been reported to design, fabricate, and experimentally test the gas-cooled leads mainly for 4–5 K magnets, the details of technical information or optimized data are barely available for 20 K leads, so far as the authors are aware. This study is proposed to rigorously investigate the thermal characteristics of gas-cooled current leads with contemporary REBCO tapes. In particular,

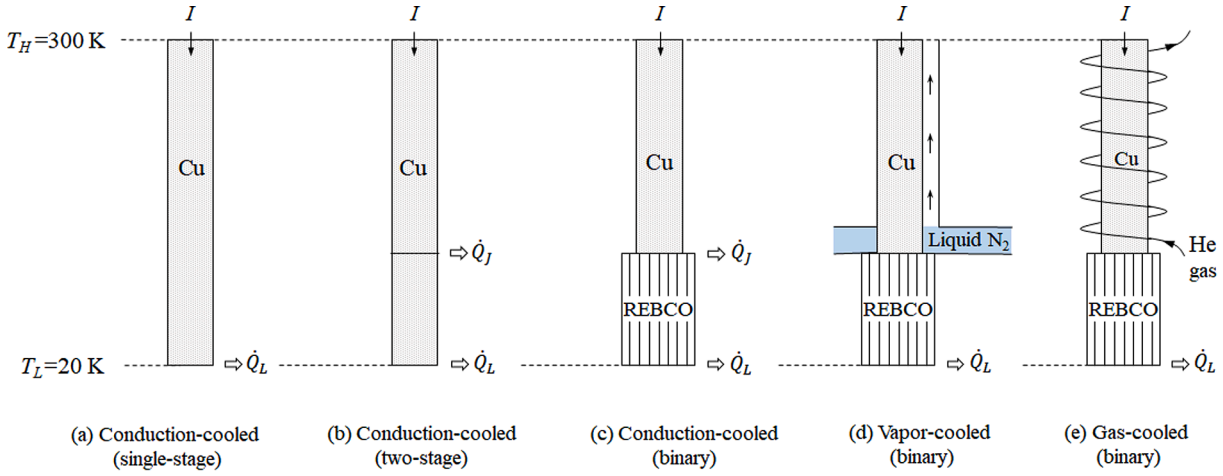

Fig. 1. Five different options of current leads for superconducting magnets at 20 K.

it is intended to examine the thermodynamic nature of two refrigeration requirements (i.e. the cryogenic refrigeration of REBCO at 20 K and the continuous convective gas-cooling of Cu), and to devise an optimization scheme applicable to 10–30 kA leads for emerging high-field HTS magnets at 20 K.

2. Analysis and optimization

2.1. Formulation

The configuration of a gas-cooled current lead for 20 K magnets is schematically shown in Fig. 2. The cold end of REBCO tapes is maintained at 20 K, and Cu conductor is convectively cooled by the forced-flow of He gas from the joint at T_J to the warm end at 300 K. In steady state, the energy balance equation is

$$\frac{d}{dx}\left(k_1 A_1 \frac{dT_1}{dx}\right) = 0 (0 \le x \le L_1) \tag{1}$$

for REBCO tapes, assuming that there is no heat generation, and

$$\frac{d}{dx}\left(k_2 A_2 \frac{dT_2}{dx}\right) + \frac{\rho_2 I^2}{A_2} - hP_e\left(T_2 - T_g\right) = 0 (L_1 \le x \le L_1 + L_2) \tag{2}$$

$$-\dot{m} C_p \frac{dT_g}{dx} + hP_e\left(T_2 - T_g\right) = 0 (L_1 \le x \le L_1 + L_2) \tag{3}$$

for Cu conductor and He gas, respectively. Throughout the paper, the subscripts 1, 2, and g denote REBCO tapes, Cu conductor, and He gas, respectively. The axial distance, x, is measured from cold end, and A and L are the cross-sectional area and axial length of conductors, respectively. ρ and k are the electrical resistivity and thermal conductivity, respectively, and hP_e is the product of convection heat transfer coefficient and effective perimeter, as described later.

Two boundary conditions are given as the end temperatures.

$$T_1(0) = T_L = 20 \text{ K} \tag{4}$$

$$T_2(L_1 + L_2) = T_H = 300 \text{ K} \tag{5}$$

The inlet temperature of He gas is an important design parameter.

$$T_g(L_1) \equiv T_{gi} \tag{6}$$

A good connection of REBCO and Cu is crucial for electrical and thermal conduction as well as for mechanical strength. For simplicity, it is assumed that temperature is continuous and the resistive heating is negligibly small at the soldering joint.

$$T_1(L_1) = T_2(L_1) \equiv T_J \tag{7}$$

$$k_1 A_1 \frac{dT_1(L_1)}{dx} = k_2 A_2 \frac{dT_2(L_1)}{dx} \tag{8}$$

There is no extra heat intercept at the joint, but only the Cu conductor is convectively cooled by He gas.

From thermodynamic point of view, there are two distinct requirements for refrigeration in order to maintain the system at steady state: (1) the removal of thermal load at T_L = 20 K and (2) the continuous cooling of He gas from T_{ge} back to T_{gi}. By combining the first and second laws of thermodynamics [1], the input power (work) for refrigeration is derived.

$$\dot{W} \ge \dot{W}_{rev} = \dot{Q}_L\left(\frac{T_H}{T_L} - 1\right) + \dot{m}[(i_i - i_e) - T_H(s_i - s_e)]$$
$$= \frac{k_1 A_1}{L_1}(T_J - T_L)\left(\frac{T_H}{T_L} - 1\right) + \dot{m} C_p\left(T_{gi} - T_{ge} - T_H \ln\frac{T_{gi}}{T_{ge}}\right) \tag{9}$$

where T_H is the ambient temperature (300 K) where heat is rejected, and i and s are the specific enthalpy and entropy of He gas, respectively. $\dot{W}_{rev}$ is the reversible work for refrigeration [1], where the term "reversible" means that there is no entropy generation in the process. The second term of right-handed side in Eq. (9) is the difference of flow availability (or exergy) between inlet and exit of He gas, and it is assumed that the effect of pressure drop on refrigeration is negligible. The specific heat of He (C_p) is nearly constant over 20–300 K at a moderately low pressure (<1 MPa) [33], but the thermal conductivity of REBCO tapes (k_1) should be averaged for accuracy between T_L (20 K) and T_J. In practice, modified Brayton cycles should be employed for this refrigeration [34], and the state-of-the-art turbo-Brayton refrigerators have a value of FOM (figure of merit or so-called percentage Carnot) around at 0.20–0.25 [34–36]. The key point here is that even though the actual input power may be 4 or 5 times greater than the reversible work, the current leads could be optimized so as to minimize the reversible work.

2.2. Properties of conductors

REBCO tape is a thin composite material, and many different products are now commercially available from several manufactures. As recommended for current-lead application by SuNAM [37], an example of the cross-section is shown in Fig. 3. The apparent axial thermal conductivity, k_1, is an area-weighted average of component materials, which is approximately 90–170 W/m-K at 20–100 K. As mentioned above, the heat flow through the stacks of REBCO tapes ($\dot{Q}_L$) in Fig. 2 can be calculated with temperature-averaged k_1 between T_L (20 K) and T_J from Eq.(1).

The superconducting properties of REBCO tape are provided by manufacturers as well. For the tape in Fig. 3, the critical temperature (T_C) is 92 K, and the self-field critical current at 77 K is 150 A. Since the REBCO temperature is highest at the joint, the critical current at T_J will play an essential role in this optimization. As discussed later, the joint temperature is in the range of 50–80 K, and the linear model is a good approximation for I_C as a function of T_J.

$$I_C(T_J) \approx I_C(77 \text{ K}) \cdot \left(\frac{T_C - T_J}{T_C - 77}\right) = 10(92 - T_J)\ [A] \quad (50 \text{ K} \le T_J \le 80 \text{ K}) \tag{10}$$

Copper is a widely used metal for cryogenic current leads. Thermal conductivity (k_2) and electrical resistivity (ρ_2) of pure Cu are strongly dependent on RRR (residual resistivity ratio) at temperatures below

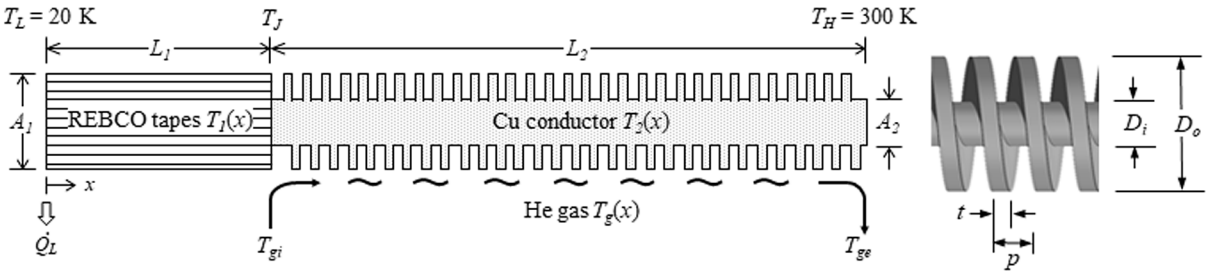

Fig. 2. Configuration of a gas-cooled current lead with REBCO tapes and spiral-fin Cu conductor.

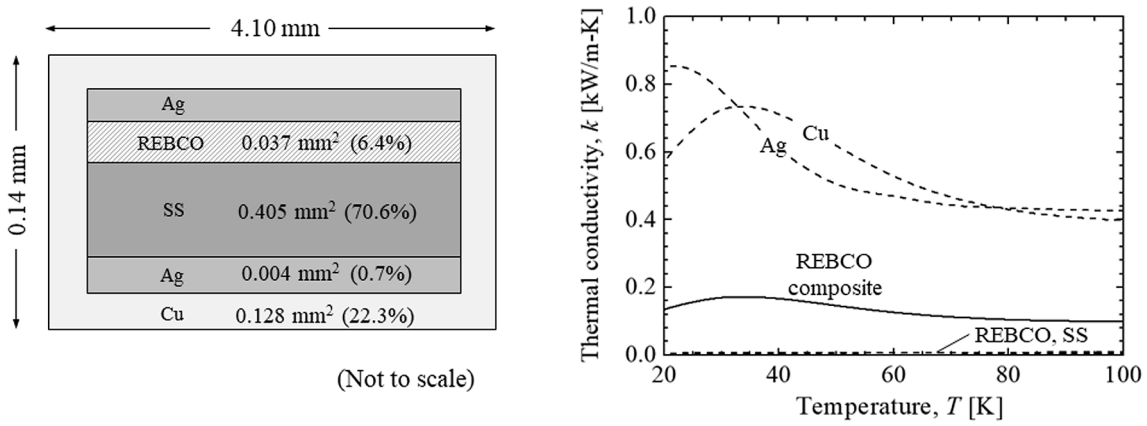

Fig. 3. Schematic cross-section of a commercial REBCO tape [37] and apparent axial thermal conductivity as a function of temperature.

100 K [38–40], as shown in Fig. 4. In general, small RRR is preferred for low thermal conductivity, while large RRR is preferred for small electrical resistivity. In case of a perfect Wiedemann-Franz material, the product of k and ρ is constant, regardless of RRR. For Cu, however, there is some deviation from the Wiedemann-Franz law, and the temperature-dependent properties are numerically incorporated into analysis and optimization.

2.3. Convection heat transfer and effective perimeter

In many vapor-cooled or gas-cooled leads for large current over 10 kA, Cu conductor with spiral fin has been used to augment the convective cooling [14.17,18,25,27,30–32]. The spiral fin is machined around a cylindrical rod so that the He gas flows helically along rectangular cooling channel. The hydraulic diameter of the rectangular channel is given by

$$d = \frac{2(D_o - D_i)(p - t)}{(D_o - D_i) + 2(p - t)} \tag{11}$$

where D_o, D_i , p, and t are the outer and inner diameter, axial pitch, and thickness of spiral fin, respectively, as indicated in Fig. 2. Assuming that the inertial (centrifugal) effect of He flow is negligible, the convection heat transfer coefficient can be calculated from the Colburn equation for non-circular ducts [41]. For turbulent flow in the rectangular channel,

$$h = 0.023 \frac{k_g}{d} \left(\frac{4\dot{m}}{\mu[(D_o - D_i) + 2(p - t)]} \right)^{0.8} \sqrt[3]{Pr} \tag{12}$$

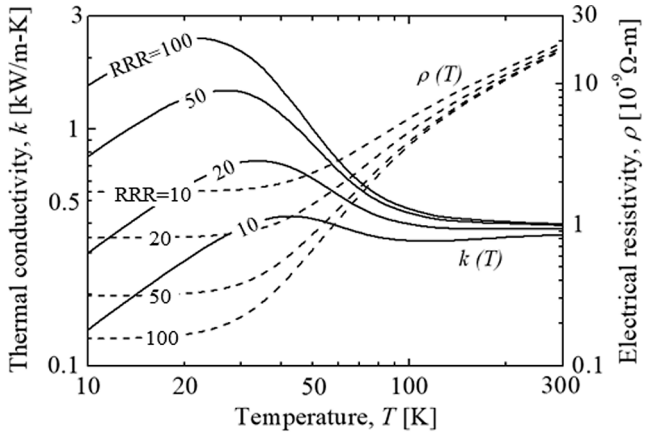

Fig. 4. Thermal conductivity and electrical resistivity of copper as a function of temperature [38].

where μ and Pr are the viscosity and Prandtl number of He gas, respectively, and the term in parenthesis is the Reynolds number (Re). The effective perimeter is defined by

$$P_e = P\left[1 - \frac{P_f}{P}(1 - \eta_f)\right] = \frac{\pi}{2p}\left[2D_i(p - t) + \left(D_o^2 - D_i^2\right)\right]\left[1 - \frac{D_o^2 - D_i^2}{2p(D_i - 2t) + \left(D_o^2 - D_i^2\right)}(1 - \eta_f)\right] \tag{13}$$

where P is the total perimeter of cooling gas at an axial location and P_f is the perimeter of fin or extended surface, as derived earlier by Chang et al. [31]. The fin efficiency, η_f, for radial fin is calculated with an explicit expression of modified Bessel functions [31,41].

2.4. Design parameters and numerical method

A number of specifications and properties are involved in this analysis and optimization. Two end temperatures are fixed in Eq.(4) and (5) as boundary conditions, and the operation current, I, is specified in the range of 10–30 kA. The material properties are needed for the apparent k_1 and I_C of REBCO tape and the RRR value of Cu.

In order to solve the systems of equations, six design parameters should be given, including four geometric factors of conductors (L_1, A_1, L_2, A_2) and two gas cooling factors of He (T_{gi}, $\dot{m}$). The cross-sectional area of REBCO stack is determined by the superconducting capacity of stacked tapes. As no resistive heating is assumed in Eq.(1), the optimization is subject to a constraint

$$I \le N \cdot I_C(T_J) \tag{14}$$

where N is the number of REBCO tapes and I_c is the critical current of single REBCO tape at T_J. In theory, the thermal load at T_L could be smallest with the minimum N (or the minimum A_1), as demonstrated in the optimization of conduction-cooled HTS leads [9]. In practice, however, the actual N should be determined with a certain safety margin. For example, if the leads are designed for operation at 50% level of the critical current at T_J.,

$$N = \frac{I}{0.5 \times I_C(T_J)} = \frac{2I}{I_C(T_J)} \tag{15}$$

Since N is determined, the number of parameters is now reduced to five (L_1, L_2, A_2, T_{gi}, $\dot{m}$) so that Eq.(1)-(3) can be numerically solved with these five given values. Since the boundary conditions are imposed at two ends, the differential equations should be solved by trial-and-error (so-called the shooting) method. The fourth-order Runge-Kutta method is used as numerical integration scheme. From the numerical solution, the joint temperature (T_J) and the exit temperature of He (T_{ge})

are obtained for Eq.(9) to calculate and minimize the reversible work for refrigeration.

3. Results and discussion

3.1. Temperature profile and joint temperature

In order to demonstrate the optimization procedure, the specifications and properties of 10 kA gas-cooled binary leads are listed in Table 1. Among the five design parameters (L_1, L_2, A_2, T_{gi}, $\dot{m}$), the length is selected first as $L_1 = 0.4$ m (REBCO tapes) and $L_2 = 0.6$ m (Cu conductor). The system of equations is solved numerically to find three temperature distributions of REBCO, Cu, and He (T_1, T_2, T_g) with the given values of three parameters (A_2, T_{gi}, $\dot{m}$). The fin dimension in Table 1 is selected in reference to the previous papers [14.18,25,30–32].

The temperature is plotted for REBCO, Cu, and He in Fig. 5 for the case of $A_2 = 8.2$ cm^2, $T_{gi} = 50$ K, $\dot{m} = 0.8$ g/s. The temperature profile is almost linear for REBCO, but convex downward for Cu. Near the joint ($x = 0.4$ m), He temperature (T_g) is much lower than Cu temperature (T_2), because of the heavy cooling load at the joint to meet the boundary condition, Eq.(8). The temperature difference between T_2 and T_g gets smaller rapidly and then larger again along the He flow up to warm end. As result, T_J and T_{ge} are 70 K and 258 K, respectively.

For comparison, the dashed and dotted curves are additionally plotted in Fig. 5. The dashed curve is the temperature profile of an optimized conduction-cooled binary lead shown in Fig. 1(c), and the dotted curve is the temperature profile of gas-cooled binary lead with "perfect" heat transfer between Cu and He. In the conduction-cooled lead, the temperature gradient is zero at warm end. The amount of heat intercept in the conduction-cooled lead is determined by the difference in the heat flow from Cu and the heat flow to REBCO at the joint. In case of perfectly gas-cooled lead, temperature is same for Cu and He at any axial location, and the temperature gradient at the joint is much smaller.

Table 1
Specifications and properties of gas-cooled binary leads to demonstrate the optimization.

Specifications	Warm end temperature	T_H	300 K
	Cold end temperature	T_L	20 K
	Operating current	I	10 kA
Properties	Critical current of REBCO	I_C (77 K)	150 A
	RRR of Cu		50
	Specific heat of He	C_p	5.19 kJ/kg-K
Fin dimension	Fin height	$(D_o - D_i)/2$	3 cm
	Fin thickness	t	3 mm
	Fin pitch	p	7 mm

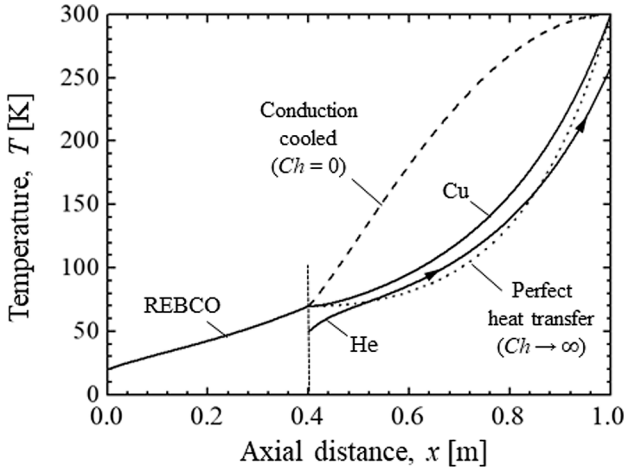

Fig. 5. Calculated temperature profile of REBCO, Cu, and He ($A_2 = 8.2$ cm^2, $\dot{m} = 0.8$ g/s, $T_{gi} = 50$ K).

The same calculation is repeated with various values of T_{gi} and $\dot{m}$, and the results are plotted in Fig. 6. The dot in the graphs indicates the specific case of Fig. 5. Two graphs in Fig. 6 contain the exactly same information, because Fig. 6(a) is a graphic display of $T_J = f(\dot{m}, T_{gi})$ and Fig. 6(b) is a graphic display of $\dot{m} = f(T_J, T_{gi})$ from one data set. The former is regarded as the "operation" standpoint in a sense that the flow rate and inlet temperature of He are the actual cooling condition. On the other hand, the latter is regarded as the "design" standpoint in a sense that the required He flow rate is determined for the intended T_J. Since there is one-to-one correspondence between $\dot{m}$ and T_J, the design standpoint is adopted for convenience in this study, so the three design parameters are (A_2, T_{gi}, T_J) instead of (A_2, T_{gi}, $\dot{m}$) from now on.

3.2. Optimization of Cu Cross-sectional area and He inlet temperature

The reversible work for refrigeration is plotted in Fig. 7 as a function of Cu cross-sectional area (A_2) and He inlet temperature (T_{gi}) for various values of joint temperature (T_J). For a given T_J, there exists a unique optimum (indicated by dots) for A_2 and T_{gi} to minimize the reversible work. The optimum A_2 is the point of balance between heat conduction and Joule heating, similarly with conduction-cooled leads. A smaller A_2 results in more work due to excessive Joule heating, and a larger A_2 results in more work due to excessive heat conduction. The existence of optimal T_{gi} was reported earlier in the gas-cooled binary leads for ITER magnets [13]. A lower T_{gi} needs more power due to excessively low temperature, and a higher T_{gi} needs more power due to excessively large flow rate.

In all cases, the reversible work decreases as T_J increases, which means that a higher T_J (with the corresponding larger optimum A_2) is preferred for efficient refrigeration. As T_J increases, on the other hand, the required number of REBCO tapes (N) increases in accordance with Eq. (15), and the temperature margin for superconductivity becomes narrow, affecting the thermal stability and protection against the quench. The selection of T_J is therefore a typical engineering decision, taking into account the efficiency, the capital cost, the manufacturability, and the operational stability.

The slope of curves in Fig. 7 has a significant implication in practical design. In Fig. 7(a), the curves are relatively steep in the left region of optimum, but rather gradual in the right region. This means that any under-design in Cu cross-sectional area should be cautiously avoided. In Fig. 7(b), on the contrary, the curve is relatively gradual in the left region of optimum, but steep in the right region. This means that any over-design in He inlet temperature should be cautiously avoided.

The optimal conditions of gas-cooled leads are compared with those of conduction-cooled leads. Fig. 8 shows the reversible work as a function of A_2 for gas-cooled and conduction-cooled leads. The overall behavior looks similar, but the optimum A_2 and the corresponding W_{rev} are much smaller in gas-cooled leads for the same joint temperature and conductor length. It can be generally stated that the gas-cooling is superior to the conduction-cooling in terms of thermodynamic efficiency.

It is interesting to examine the temperature difference between Cu conductor and He gas. Fig. 9(a) compares the temperature profile in two optimized cases ($T_J = 80$ K and 50 K), and Fig. 9(b) highlights the temperature difference ($T_2 - T_g$) in four cases ($T_J = 50$–80 K). As noted earlier, the temperature difference is large (15–25 K) at the joint ($x = 0.4$ m), sharply drops to a minimum (6–9 K) around at $x = 0.5$ m, and then increases gradually to the warm end. Even though the temperature levels are different each other for $T_J = 50$–80 K, the four curves of temperature difference are closely overlapped in the middle section of gas-cooled Cu ($x = 0.6$–0.8 m), and disperse towards the warm end, depending on T_J. Recalling that the magnitude of convection heat is basically proportional to the temperature difference, it can be stated that the gas-cooling rate is relatively more active near the joint and the warm

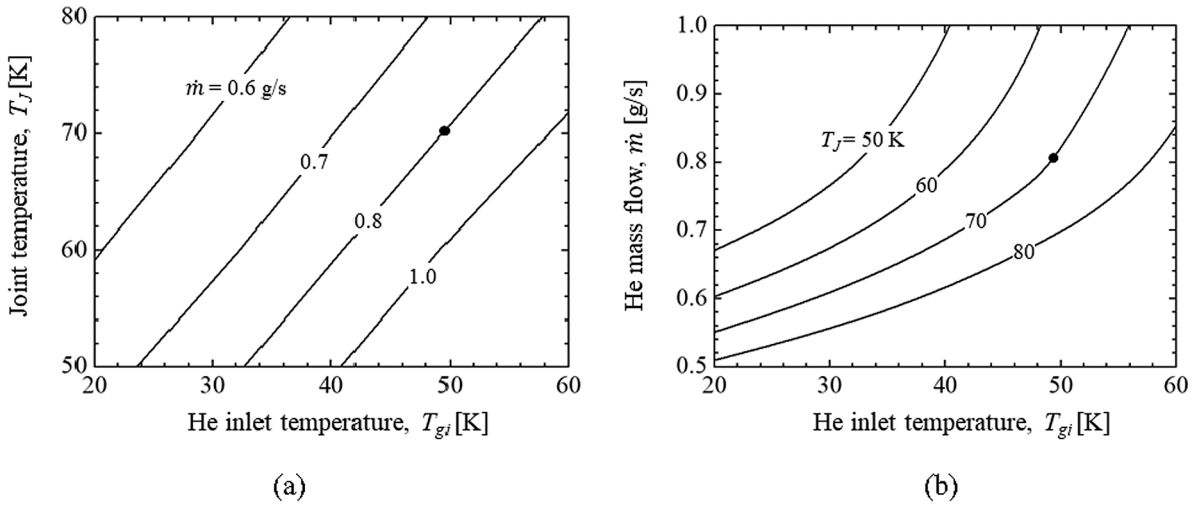

Fig. 6. Joint temperature and He mass flow rate as a function of He inlet temperature.

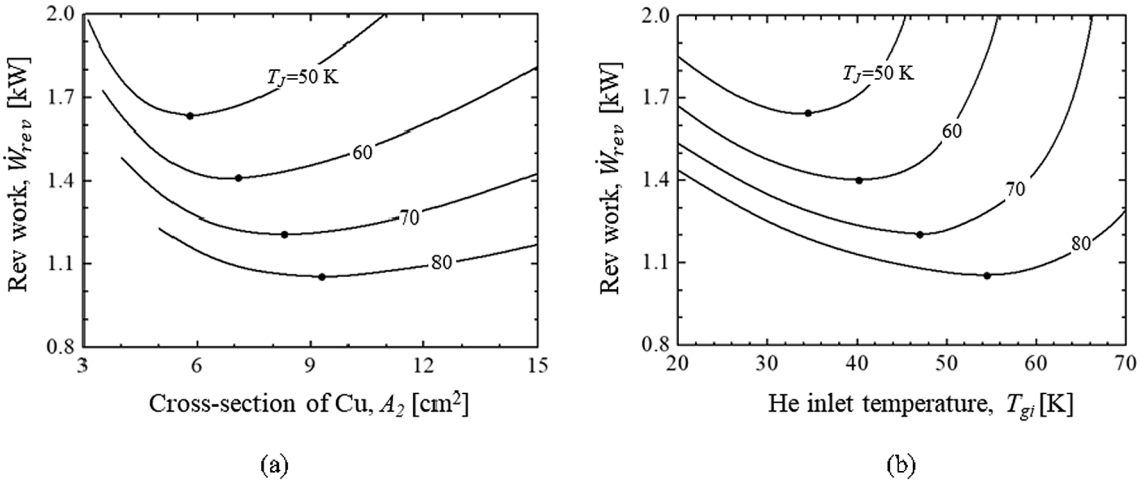

Fig. 7. Reversible work for various values of joint temperature: (a) as a function of Cu cross-sectional area with optimized He inlet temperature at the given T_J, (b) as a function of He inlet temperature with optimized Cu cross-sectional area at the given T_J.

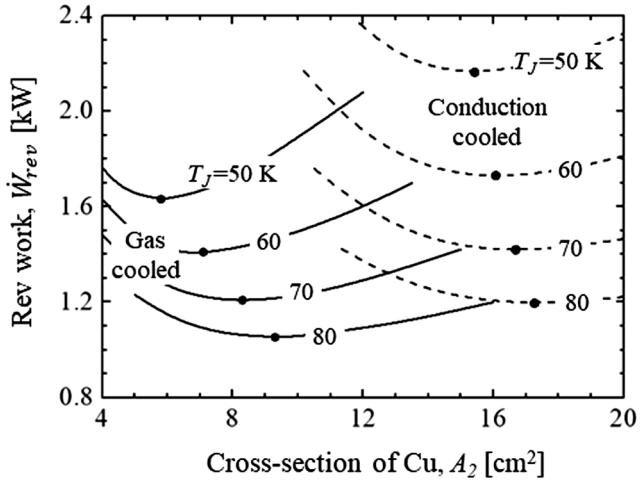

Fig. 8. Comparison of gas-cooled and conduction-cooled leads in terms of reversible work as a function of Cu cross-sectional area with optimized He inlet temperature at the given joint temperature.

end.

The effect of convective cooling on lead design was discussed earlier in terms of a dimensionless number *Ch*, called the convective heat transfer (or Chang) number [31]. The *Ch* number is an index to indicate the relative ratio of convective cooling to Joule heating at an axial location of conductor, defined as

$$Ch \equiv \frac{hP_e k_2 A_2}{I^2 L_0} \tag{16}$$

where L_0 is the Lorenz number or the product of k_2 and ρ_2 divided by absolute temperature. As noted in Fig. 5, the limiting case of $Ch = 0$ is a conduction-cooled lead (the adiabatic limit), and the other limiting case of $Ch = \infty$ is a "perfectly" gas-cooled lead where the gas and conductor temperatures are same at any axial position (the isothermal limit). Since the values of *Ch* number are much greater than unity (10–15) (as presented in the last section), the gas-cooling is considered to be quite effective in these optimized cases.

3.3. Thermodynamic evaluation

Fig. 10 compares the reversible work for the five different options in Fig. 1. In every case, the dimensional size of conductors and the cooling conditions, if any, are optimized at 10 kA. In case of (a) single-stage

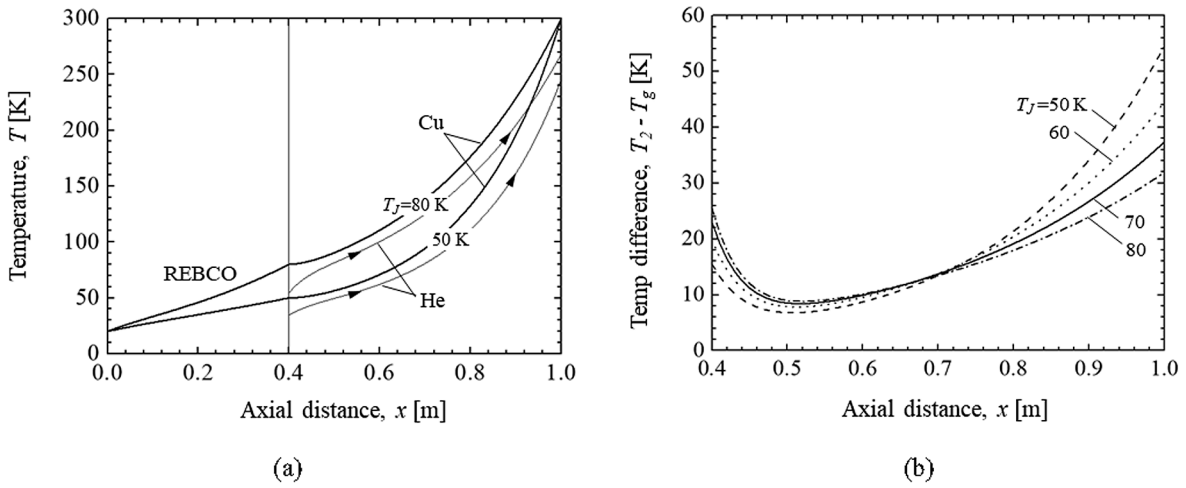

Fig. 9. Temperature profile of REBCO, Cu, and He gas when T_J = 80 K and 50 K, and highlighted temperature difference between Cu and He (optimized He inlet temperature and optimized Cu cross-sectional area for the given joint temperature).

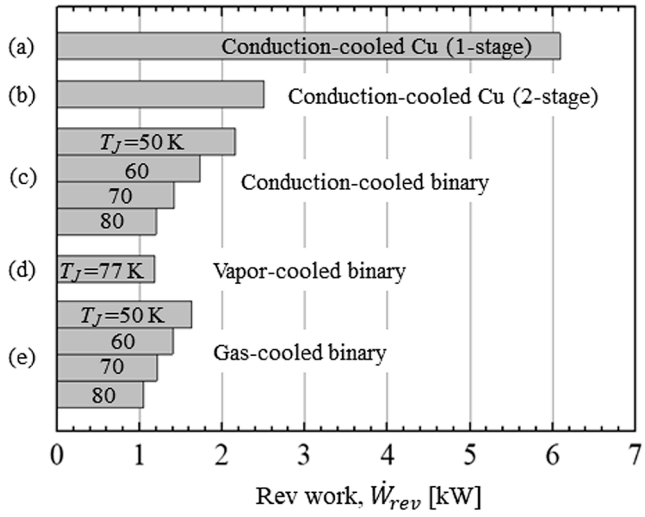

Fig. 10. Thermodynamic comparison of the five different options for 10 kA current leads in Fig. 1.

conduction-cooled Cu, the minimum work is uniquely determined at 6.09 kW, if the ratio of L/A is optimized. In case of (b) two-stage conduction-cooled Cu, the minimum work is 2.51 kW (41%), when the dimensional size of two sections and the intercept temperature are optimized. The refrigeration work could be considerably reduced by adding only one stage of heat intercept at the optimized location and temperature.

A binary lead with HTS conductor enables further reduction in the reversible work. In case of (c) conduction-cooled binary (REBCO + Cu), the minimum reversible work is 1.20–2.16 kW (20–35%), when the joint temperature T_J = 80–50 K and the cross-sectional area of Cu is optimized for L_1 = 0.4 and L_2 = 0.6 m. Similarly with the gas-cooled leads, the selection of T_J is a typical design issue, as discussed above. In case of (d) vapor-cooled binary (REBCO + Cu), T_J is fixed at liquid-nitrogen temperature (77 K), and the reversible work is uniquely determined at 1.18 kW (19%).

In case of (e) gas-cooled binary (REBCO + Cu), the reversible work is 1.05–1.63 kW (17–27 %), as presented in the previous sections. It is obvious from the comparison that the gas-cooling with T_J = 70–80 K is an excellent choice in terms of thermodynamic efficient. It should be mentioned again that the heat intercept for conduction-cooling in the cases of (b) and (c) is feasible only when the current level is low (under 1 kA) and that the vapor-cooling requires a sufficient size of liquid container and the continuous liquid supply. For a high current over 10 kA, the gas-cooling of binary leads could be a reasonably good option in efficiency as well as in feasibility to realize the closed-cycle refrigeration in practice.

3.4. Design data of 10–30 kA Gas-Cooled leads

As summary, some design data are presented for 10–30 kA gas-cooled leads, as listed in Table 2. For a specified I, three parameters should be selected for L_1, L_2, and T_J. Generally speaking, L_1 may be suggested in 0.3–0.4 m, because any longer one has only a minor effect in reducing the cooling requirement. On the other hand, L_2 is directly related with the optimal conditions and should be carefully and iteratively selected. T_J may be suggested in 50–80 K. The total length (L_1 + L_2) is 1 m in all cases of Table 2.

With three parameters, A_1 (or N) is determined by Eq.(14) and (15), and A_2 (or D_i) and T_{gi} (or $\dot{m}$) are uniquely optimized from the numerical results. The details of gas flow and fin parameters are listed, including the fin efficiency (η_f) and dimensionless numbers (Re and Ch). In all cases, turbulent flow can be confirmed with Re. It is noted that unlike conduction-cooled leads, the optimal condition of gas-cooled leads is not simply given by the L_2/A_2 ratio. At the bottom of Table 2, the reversible work for refrigeration is listed in each optimized case. Since the reversible work is expressed as sum of two terms in Eq. (9), each value is listed as (Cold end) and (He gas). The contribution of cold-end refrigeration is only 0.4–3.8% of total work, because of the low thermal conductivity of REBCO tapes.

The effect of pressure drop of He gas flow is mentioned with the optimized data in Table 2. The reversible work for refrigeration was calculated in Eq. (9) without the pumping power against the pressure drop loss. In the spiral fin or other feasible shapes of gas-cooled Cu conductor, the pressure drop may be estimated in the range of 30–100 kPa, depending on the flow rate and geometric conditions. If this is taken into account, the reversible work in Table 2 could increase up to a few percent. On the other hand, the main point in this study is that the pressure drop has only a minor effect on the optimized conditions of gas-cooled leads.

Finally, the selection of L_1, L_2, and T_J is discussed again with the design data in Table 2. In theory, the gas-cooled leads can be optimized for "any" values of L_1 and L_2, but the three cases of (0.40 + 0.60) m, (0.35 + 0.65) m, and (0.30 + 0.70) m are presented here for 10 kA, 20 kA, and 30 kA, respectively. As a matter of fact, these values have been selected after a number of trials with practical design consideration. The main reason for selecting the longer Cu length at higher current is to

Table 2
Selected design data of 10–30 kA gas-cooled binary leads with REBCO tapes.

Specified	I	10 kA				20 kA				30 kA			
Selected	L_1 [m]	0.40				0.35				0.30			
	L_2 [m]	0.60				0.65				0.70			
	T_J [K]	50	60	70	80	50	60	70	80	50	60	70	80
Designed or Optimized	A_1 [cm^2]	0.28	0.36	0.52	0.96	0.55	0.72	1.04	1.92	0.82	1.08	1.57	2.87
	A_2 [cm^2]	5.8	7.1	8.3	9.3	12.7	15.4	17.8	20.0	20.4	24.8	28.6	32.1
	T_{gi} [K]	34.5	40.2	47.0	54.5	34.8	40.8	47.6	55.1	35.1	41.1	48.1	55.7
Detailed	N	48	63	91	167	96	125	182	334	143	188	273	500
	D_i [cm]	2.72	3.01	3.25	3.44	4.02	4.43	4.76	5.05	5.10	5.62	6.03	6.39
	$\dot{m}$ [g/s]	0.83	0.79	0.76	0.75	1.61	1.54	1.49	1.46	2.36	2.26	2.19	2.14
	T_{ge} [K]	245	255	263	268	251	261	268	273	254	266	272	277
	Re	13500	12100	11200	10600	25800	23400	21600	20400	37400	33900	31500	29800
	h [W/m^2-K]	52.0	50.4	49.4	48.9	88.8	86.3	84.5	83.6	121	117	115	114
	η_f	0.958	0.960	0.961	0.962	0.938	0.940	0.942	0.943	0.923	0.925	0.927	0.928
	P_e [m]	1.52	1.61	1.68	1.73	1.85	1.96	2.06	2.14	2.11	2.25	2.37	2.47
	Ch	10.2	12.0	13.8	15.5	11.6	13.6	15.6	17.6	12.8	15.2	17.5	19.7
	$\dot{W}_{rev}$ [kW]	1.63	1.40	1.21	1.05	3.16	2.71	2.33	2.05	4.62	3.96	3.41	3.00
	(Cold end)	(0.01)	(0.01)	(0.02)	(0.03)	(0.01)	(0.02)	(0.03)	(0.07)	(0.02)	(0.03)	(0.05)	(0.11)
	(He gas)	(1.62)	(1.39)	(1.19)	(1.02)	(3.15)	(2.69)	(2.30)	(1.98)	(4.60)	(3.93)	(3.36)	(2.89)

provide more cooling surface and avoid an excessively large flow rate of He gas. The table shows quantitatively how much the required work can be reduced, as T_J increases. On the other hand, as T_J increases, both the required number of REBCO tapes and the diameter of Cu conductor dramatically increase as well, which could bring more difficulty in fabrication for the reliable joint and uniform current density. In addition, the thermal stability could be worse with higher T_J, as discussed above. Among the design data in Table 2, it may be suggested to select a relatively high T_J for 10 kA and a relatively low T_J for 30 kA, as indicated by gray background. It is noticeable that the Ch number is around 13 in the three cases of suggested design.

4. Conclusions

A comprehensive thermodynamic optimization is presented for gas-cooled binary current leads with REBCO tapes, aiming at the upcoming application to high-field HTS magnets at 20 K. The temperature distributions of Cu conductor and cooling He gas are rigorously calculated with the temperature-dependent properties and estimated convection heat transfer with spiral fin. From the results of numerical analysis, the work requirement for refrigeration is calculated for various values of design parameters. It is proven that there exist optimal conditions for the cooling gas (temperature and flow rate) and the dimensional size of conductors to minimize the refrigeration work. The key parameter in the design is the joint temperature between REBCO and Cu, which should be selected in the range of 50–80 K, taking into consideration the efficiency of refrigeration and other practical factors such as manufacturability and operational stability. Even though there are a number of important technical issues in designing the gas-cooled leads with REBCO tapes for 10–30 kA application, this optimization could be a theoretical basis for the dimensional size and cooling gas conditions.

CRediT authorship contribution statement

Ho-Myung Chang: Supervision, Conceptualization, Writing – original draft. **Na Hyeon Kim:** Data curation, Visualization, Writing – review & editing. **Sangjun Oh:** Project administration, Funding acquisition, Writing – review & editing.

Declaration of Competing Interest

The authors declare that they have no known competing financial interests or personal relationships that could have appeared to influence the work reported in this paper.

Data availability

Data will be made available on request.

Acknowledgments

This research is supported by National R&D Program through the National Research Foundation of Korea (NRF) funded by Ministry of Science and ICT (2022M3I9A1076800).

References

[1] Bejan A. Advanced Engineering Thermodynamics. John Wiley & Sons Inc; 2016.
[2] Wilson MN. Superconducting magnets. Oxford: Clarendon Press; 1987.
[3] Weisend II JG. Handbook of Cryogenic Engineering. Philadelphia: Taylor & Francis; 1998.
[4] Buyanov YL, Fradkov AB, Shebalin IY. A review of current leads for cryogenic devices. Cryogenics 1975;15(4):194–200.
[5] Hilal MA. Optimization of Current Leads for Superconducting Systems. IEEE Trans Magnetics 1977;MAG-13(1):690–3..
[6] Buyanov YL. Current leads for use in cryogenic devices. Principle of design and formulae for design calculations. Cryogenics 1985;25(2):94–110.
[7] Herrmann PF, Cottevieille C, Duperray G, Leriche A, Verhaege T, Albrecht C, et al. Cryogenic load calculation of high Tc current lead. Cryogenics 1993;33(5):555–62.

[8] Wesche R, Fuchs AM. Design of superconducting current leads. Cryogenics 1994;34(2):145–54.
[9] Chang HM, Van Sciver SW. Thermodynamic optimization of conduction-cooled HTS current leads. Cryogenics 1998;38(7):729–36.
[10] Chang HM, Van Sciver SW. Optimal Integration of Binary Current Lead and Cryocooler. Cryocoolers 2002;10:707–16.
[11] Miller JR, Miller GE, Kenny SJ, Windham RDE, Cl.. Design and development of a pair of 10 kA HTS current leads for the NHMFL 45T hybrid magnet system. IEEE Trans Appl Supercond 2005;15(3):1492–5.
[12] Xie YY, Knoll A, Chen Y, Li Y, Xiong X, Qiao Y, et al. Progress in scale-up of second-generation high-temperature superconductors at SuperPower Inc. Physica C: Superconductivity and its Applications 2005;426–431, Part 2,:849-57.
[13] Wesche R, Heller R, Bruzzone P, Fietz WH, Lietzow R, Vostner A. Design of high-temperature superconductor current leads for ITER. Fusion Eng Des 2007;82(5–14):1385–90.
[14] Ballarino A. Large-capacity current leads. Physica C 2008;468(15–20):2143–8.
[15] Fleshler S, Buczek D, Carter B, Cedrone P, DeMoranville K, Gannon J, et al. Scale-up of 2G wire manufacturing at American Superconductor Corporation. Physica C 2009;469(15–20):1316–21.
[16] Fietz WH, Heller R, Kienzler A, Lietzow R. Status of HTS current leads for WENDELSTEIN 7-X and JT-60SA. Fusion Eng Des 2009;84(2–6):776–9.
[17] Wesche R, Borsch M, Bruzzone P, Holdener F, Iten E, Magginetti N, et al. Development of HTS Current Leads for Industrial Fabrication. IEEE Trans Appl Supercond 2012;22(3):4800304.
[18] Wesche R, Borsch M, Bruzzone P, Holdener F, Iten E, Magginetti M, et al. Design of the HTS Current Leads for ITER. IEEE Trans Appl Supercond 2012;22(3):4801004.
[19] Marshall WS, Bird MD, den Ouden A, Dixon IR, Lu J, Petenboom AAJ, et al. Fabrication of HTS Conductor Stacks for 2-kA Binary Current Leads for MagLab Series-Connected Hybrid and HFML Nijmegen Hybrid Magnets. IEEE Trans Appl Supercond 2015;25(3):4801704.
[20] Zhou T, Lu K, Ding K, Song Y. Design and Development of 16-kA HTS Current Lead for HMFL 45-T Magnet. IEEE Trans Appl Supercond 2015;25(4):4802906.
[21] Bonura M, Senatore C. High-field thermal transport properties of REBCO coated conductors. Supercond Sci Technol 2015;28:025001.
[22] Kovalev IA, Surin MI, Naumov AV, Novikov MS, Novikov SI, Ilin AA, et al. Test results of of 12/18 kA ReBCO coated conductor current leads. Cryogenics 2017;85:71–7.
[23] Zappatore A, Heller R, Savoldi L, Zanino R. Test results of a 20 kA high temperature superconductor current lead using REBCO tapes. Cryogenics 2018;95:95–101.
[24] Heller R, Fietz WH, Groner F, Heiduk M, Mollik M, Lange C, et al. Assessment of the performance of a 20 kA REBCO current lead. Supercond Sci Technol 2018;31:055014.
[25] Zhang S, Feng H, Zhuang M, Ding K, Liu C, Zhou Y. Experimental Research of a 10 kA HTS Current Lead Using YBCO Tapes. IEEE Trans Appl Supercond 2020;30(8):4801307.
[26] Heller R, Fietz WH, Hamada K, Murakami H, Wanner M. Overview and first operation of the high temperature superconductor current leads during integrated commissioning of JT-60S. Fusion Eng Des 2021;172:112910.
[27] Dong Y, Ran Q, Lu K, Zheng J, Liu C, Liu H, et al. Structure, design, and test of 13 kA HTS current lead. Cryogenics 2023. in press.
[28] Chang HM, Choi YA, Van Sciver SW. Optimization of operating temperature in cryocooled HTS magnets for compactness and efficiency. Cryogenics 2002;42(12):787–94.
[29] Yamaguchi S, Emoto M, Kawahara T, Hamabe M, Watanabe H, Ivanov Y, et al. A Proposal of Multi-stage current lead for reduction of heat leak. Phys Procedia 2012;27:448–51.
[30] Maehata K, Kawasaki S, Ishibashi K, Wakuta Y, Kawamata H, Shintomi T. Operational performance of spiral-fin current leads. Cryogenics 1993;33(7):680–5.
[31] Chang HM, Byun JJ, Jin HB. Effect of convection heat transfer on the design of vapor-cooled current leads. Cryogenics 2006;46:324–32.
[32] Polli GM, Affinito L, della Corte A. Heat Exchanger Design for the 30 kA Gas Cooled Current Leads in the ENEA 12 T CICC Facility. IEEE Transactions on Applied Superconductivity 2011;21(3):1079-83.
[33] Lemmon EW, Huber ML, McLinden MO. NIST Reference Fluid Thermodynamic and Transport Properties Database REFPROP Version 9.0 (Available at https://www.nist.gov/srd/refprop).
[34] Bromberg L, Michael P, Minervini JV, Dietz AJ. Evaluation of Turbo-Brayton Cycle for Cooling Current Leads: Integrated Current Lead/Heat Exchanger. Adv Cryog Eng 2012;57:993–1000.
[35] Chang HM, Kim SG, Weisend II JG, Quack H. Modified Brayton Refrigeration Cycles for Liquid Hydrogen in Spallation Neutron Source Moderator. Cryocoolers 2016;19:463–70.
[36] Chang HM, Park CW, Yang HS, Sohn SH, Lim JH, Oh SR, et al. Thermodynamic Design of 10 KW Brayton Cryocooler for HTS Cable. Adv Cryog Eng 2012;57:1664–71.
[37] Zhang H, Suo H, Wang L, Ma L, Liu J, Zhang Z, et al. Database of the effect of stabilizer on the resistivity and thermal conductivity of 20 different commercial REBCO tapes. Supercond Sci Technol 2022;35:045016.
[38] Cryocomp Properties Version 3.06. Distributed by Cryodata Inc. (Available at http://www.cryodata.com/).
[39] NIST-Material Properties (Available at http://cryogenics.nist.gov/).
[40] Maehata K, Ishibashi K, Wakuta Y. Design chart of gas-cooled current leads made of copper of different RRR values. Cryogenics 1994;34(11):935–40.
[41] Incropera FP, De Witt DP, Bergman TL, Lavine AS. Fundamentals of Heat and Mass Transfer. 6th ed. New York: John Wiley & Sons; 2006.